Neurobiology of Disease 179 (2023) 106051

Contents lists available at ScienceDirect

Neurobiology of Disease

journal homepage: www.elsevier.com/locate/ynbdi

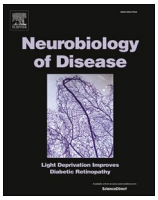

Machado Joseph disease severity is linked with gut microbiota alterations in transgenic mice

Hasinika K.A.H. Gamage [a,b,1], Katherine J. Robinson [c,1], Luan Luu [c], Ian T. Paulsen [a,b,d], Angela S. Laird [c,*]

[a] School of Natural Sciences, Macquarie University, NSW 2109, Australia
[b] ARC Training Centre for Facilitated Advancement of Australia's Bioactives, Macquarie University, NSW 2109, Australia
[c] Centre for Motor Neuron Disease Research, Macquarie Medical School, Faculty of Medicine, Health and Human Sciences, Macquarie University, NSW 2109, Australia
[d] ARC Centre of Excellence in Synthetic Biology, Macquarie University, NSW 2109, Australia

ARTICLE INFO

Keywords:
Polyglutamine repeat
Trinucleotide repeat disease
Spinocerebellar ataxia
Gut microbiota
Gut dysbiosis

ABSTRACT

Emerging evidence suggests the presence of bidirectional interactions between the central nervous system and gut microbiota that may contribute to the pathogenesis of neurodegenerative diseases. However, the potential role of gut microbes in forms of spinocerebellar ataxia, such as the fatal neurodegenerative disease Machado Joseph disease (MJD), remains unexplored. Here, we examined whether gut microbiota alterations may be an early disease phenotype of MJD. We profiled the gut microbiota of male and female transgenic MJD mice (CMVMJD135) expressing human *ATXN3* with expanded CAG repeats (133–143 CAG) at pre-symptomatic, symptomatic and well-established stages of the disease (7, 11 and 15 weeks of age, respectively). We compared these profiles with the gut microbiota of male and female wild-type (WT) littermate control mice at same ages. Correlation network analyses were employed to explore the relevance of microbiota changes to disease progression. The results demontrated distinct sex-dependent effects in disease development whereby male MJD mice displayed earlier motor impairments than female MJD mice. The gut microbiota community structure and composition also demonstrated sex-specific differences between MJD and WT mice. In both male and female MJD mice, the shifts in the microbiota were present by 7 weeks, before the onset of any symptoms. These pre-symptomatic microbial changes correlated with the severity of neurological impairments present at later stages of the disease. Previous efforts towards developing treatments for MJD have failed to yield meaningful outcomes. Our study reports a novel relationship between the gut microbiota and MJD development and severity. Elucidating how gut microbes are involved in MJD pathogenesis may offer new and efficacious treatment strategies for this currently untreatable disease.

1. Introduction

Machado Joseph disease (MJD, also known as spinocerebellar ataxia type 3) is a fatal disease that causes progressive degeneration of neurons within many regions of the central nervous system including the midbrain, brainstem, cerebellum, and spinal cord (Rüb et al., 2013; Seidel et al., 2012; Yamada et al., 2001). Patients with MJD will develop motor symptoms such as progressive ataxia, impaired balance, motor incoordination, dystonia and muscle atrophy, and additional non-motor symptoms such as eye disturbances, speech disturbances, depression, and anxiety (Lo et al., 2016; Mastammanavar et al., 2020; Rüb et al., 2013). Unfortunately, MJD decreases the quality of life for patients, with most MJD patients becoming wheelchair-dependent and requiring high levels of care before eventually succumbing to the disease (D'Abreu et al., 2010; Mastammanavar et al., 2020). MJD is reported to be the most prevalent form of inherited ataxia found globally (Durr, 2010; Ruano et al., 2014). A particularly high prevalence of MJD is found in indigenous communities in Australia, the Azores of Portugal, China and Brazil (Burt et al., 1996; Martins and Sequeiros, 2018).

MJD is caused by the inheritance of an abnormal trinucleotide (CAG)

* Corresponding author at: Associate Professor Angela Laird, Centre for Motor Neuron Disease Research, Macquarie Medical School, Faculty of Medicine, Health and Human Sciences, Macquarie University, NSW 2109, Australia.
E-mail address: angela.laird@mq.edu.au (A.S. Laird).
[1] These authors contributed equally to this work.

https://doi.org/10.1016/j.nbd.2023.106051
Received 19 December 2022; Received in revised form 6 February 2023; Accepted 18 February 2023
Available online 21 February 2023

repeat expansion within the *MJD1/ATXN3* gene on chromosome 14 (Takiyama et al., 1993). Typically, the *ATXN3* gene will contain 44 or less CAG repeats; inheritance of *ATXN3* with 45–59 CAG repeats is considered an intermediate length repeat expansion and may lead to the development of MJD, however, some patients are unaffected, whilst inheritance of *ATXN3* with 60 or more repeats is fully penetrant and pathogenic (Costa and Paulson, 2012; Maciel et al., 1995). The length of the CAG repeat expansion has been reported to impact the severity of the disease, whereby a longer CAG length is correlated with earlier disease onset, faster disease progression and earlier mortality (Durr et al., 1996; Leotti et al., 2021; Maciel et al., 1995). The gene *ATXN3* encodes the protein ataxin-3, with the CAG repeat region encoding a long string of glutamine amino acids known as the polyglutamine (polyQ) region (Costa and Paulson, 2012). The ataxin-3 protein is known to function as a de-ubiquitinating enzyme and is involved in the ubiquitin-proteosome system and transcriptional processes (Costa and Paulson, 2012). Expansion of the polyQ region within the ataxin-3 protein has been found to alter the protein conformation and function, rendering the protein susceptible to post-translational modifications and the formation of protein inclusions, a common characteristic of many neurodegenerative diseases (Costa and Paulson, 2012; Seidel et al., 2012). Further, autophagy protein quality control pathways are thought to be dysregulated in MJD patients (Onofre et al., 2016; Sittler et al., 2018). It is hypothesised that autophagy impairments would decrease degradation and clearance of formed protein inclusions or aggregates, enhancing the disease burden produced by mutant ataxin-3.

Typically, ataxin-3 positive protein inclusions are present within neuronal nuclei in areas of the central nervous system that undergo neurodegeneration in MJD (Paulson et al., 1997; Rüb et al., 2013; Schmidt et al., 1998; Seidel et al., 2012; Yamada et al., 2001). Ataxin-3 positive inclusions are most commonly found in nuclei within the brainstem, spinal cord and cerebellum (Paulson et al., 1997; Rüb et al., 2003; Rüb et al., 2013; Schmidt et al., 1998), and therefore may play a pathogenic role in MJD. However, it remains unclear whether ataxin-3 inclusions are themselves toxic, or whether mutant expanded ataxin-3 indirectly alters cell function, indirectly leading to neurodegeneration. Despite a comprehensive understanding of the genetic cause of MJD and the pathogenic mechanisms that contribute to disease burden, there are currently no available therapeutic strategies that can slow or halt the development of MJD in patients who have inherited mutant expanded *ATXN3*. Thus, it is important to identify new disease-modifiers and therapeutic avenues that could decrease disease burden.

The mammalian gastrointestinal tract is host to thousands of microbial species, including bacteria, fungi, archaea, viruses etc., which form the gut microbiota and work symbiotically within the host to maintain metabolic, immune and brain health (Cryan et al., 2019). Gut dysbiosis, altered abundance, structure or function of the gut microbiota, has been associated with metabolic and immune-related diseases, such as inflammatory bowel disease, diabetes and obesity, as well as brain disorders, including depression and autism spectrum disorder, and neurodegenerative diseases such as Parkinson's disease, Alzheimer's disease, Huntington's disease and motor neuron disease (MND) (Cryan et al., 2019; Nandwana et al., 2022; Singh et al., 2021). There is now a wealth of experimental evidence highlighting a bidirectional communication between the gut and components of the central nervous system, forming the gut-brain axis (Cryan et al., 2019; Singh et al., 2021).

Whilst it is not completely understood how neurodegenerative diseases with a genetic origin may link to gut dysbiosis and trigger neurodegeneration, clinical reports suggest that constipation is one of the earliest symptoms reported by Parkinson's disease patients, preceding the onset of neurological symptoms (Adams-Carr et al., 2016; Savica et al., 2009), and motor neuron disease (MND) patients often report gastrointestinal problems prior to the onset of neurological symptoms (Rowin et al., 2017). Similarly, reports from França Jr et al. (2010) and Yeh et al. (2005) suggest that a proportion of MJD patients may experience gastrointestinal symptoms prior to or around the onset of neurological symptoms (França Jr et al., 2010; Yeh et al., 2005). Recently, it has been demonstrated that the presence of aggregated proteins within the gut can impact gut function and aggregates can be transmitted from the gut to the brain via gut-brain axis (Braak et al., 2006; Nandwana et al., 2022; Singh et al., 2021). Challis et al. (2020) demonstrated that inoculating the duodenum wall of non-transgenic mice with alpha-synuclein pre-formed fibrils (a protein known to aggregate in Parkinson's disease) can lead to decreased faecal pellet weight and increased gut transit time, suggesting impaired gastrointestinal function (Challis et al., 2020). Further, this inoculation led to the formation of alpha-synuclein aggregates within the brain and motor deficits, mimicking Parkinson's disease phenotypes (Challis et al., 2020).

One proposed mechanism for how gut dysbiosis may lead to proteinopathy and neurodegeneration is through altered production of microbial metabolites that may induce neuroprotective or neurotoxic effects (Nandwana et al., 2022). Several research teams have reported gut dysbiosis in patients with neurodegenerative diseases including decreased microbial diversity in Huntington's disease patients (Wasser et al., 2020) and MND patients (Ngo et al., 2020; Rowin et al., 2017) and decreased levels of nicotinamide, which is a microbiota-associated metabolite, has been reported in MND patients (Blacher et al., 2019). In transgenic MND (SOD1 G93A) mice, supplementation of nicotinamide was found to ameliorate motor deficits and improve survival (Blacher et al., 2019). Interestingly, many metabolites produced within the gut, including nicotinamide and butyrate are known to produce neuroprotective effects by enhancing the activity of the autophagy pathway (Canani et al., 2011). It is plausible that changes to gut microbiota or metabolites within the gut may lead to diminished production of metabolites that have neuroprotective effects, contributing to the pathogenesis of the disease.

To date, changes in the gut microbiome have not been explored in clinical MJD patient cohorts or animal models of MJD. In this study, we aim to characterise the gut microbiota of CMVMJD135 transgenic mice expressing mutant human *ATXN3*. We hypothesise that gut dysbiosis may be a disease signature common to many neurodegenerative diseases, regardless of any underlying genetic causes. Further, we hypothesise that gut dysbiosis may be an early disease phenotype that actively drives changes within the central nervous system via the gut-brain axis, leading to neurological symptoms. This study will compare the gut microbiome of transgenic MJD mice and non-transgenic littermates (wild-type, WT) at three different timepoints of disease progression: pre-symptomatic, symptomatic and well-established stages of the disease in the same experimental animal. These three time points were selected to focus on how the gut microbiota associates with MJD development and severity rather than time points at later stages as the microbial changes then could be confounded by impaired movement and feeding. Whilst there is no clear evidence of sex-specific differences in the progression of MJD or survival (Kieling et al., 2007; Klockgether et al., 1998), a previous study by Kong et al. (2020) reported gut microbiome differences in male R6/1 mice modelling Huntington's disease that were not present in female R6/1 mice (Kong et al., 2020). Given this, we will also compare microbiota differences in male and female CMVMJD135 mice. Through characterising changes in the gut microbiota and their relevance to disease onset, we aim to enhance the understanding of disease aetiology and pathogenesis, leading to the development of new efficacious therapeutic strategies.

2. Materials and methods

2.1. Animals

All animal procedures were approved by the Macquarie University animal ethics committee (2017/044) and were performed in accordance with the Australian Code of Practice for the Care and Use of Animals for Scientific Purposes. In this study, we utilised CMVMJD135 transgenic mice, previously developed and characterized by Silva-Fernandes et al.

(2014) at the University of Minho, Portugal (Silva-Fernandes et al., 2014). CMVMJD135 mice were bred on a C57/Bl6 background and ubiquitously express human mutant (expanded) *ATXN3* under a CMV promotor at near endogenous levels (Silva-Fernandes et al., 2014). Male CMVMJD135 mice were bred with wild-type C57/Bl6 females under pathogen-free conditions at Australian Bioresources (Moss Vale, Australia). Tail tissue was collected from F1 offspring at 2–3 weeks of age for genotyping (CMV +/−). DNA from mice found to express human *ATXN3* then underwent additional sequencing and fragment analysis to confirm the inherited CAG repeat expansion. MJD animals with a repeat length of 133 to 143 CAGs were used for experiments.

MJD mice and their WT siblings were transported to Macquarie University at 4–5 weeks of age and group-housed (2–5 animals per cage). Animals were allowed to acclimate for a total of 7 days after transportation to Macquarie University before commencing experimentation. Animals were housed according to genotype and sex to minimise coprophagia-induced confounds on the gut microbiota. All animals were housed in light and temperature-controlled rooms (12-h light/dark cycle, lights on at 06:00) in exhaust-ventilated cages (125 mm (W) x 350 mm (L) x 135 mm (H)) with *ad libitum* access to food and water. All mice were fed a standard chow diet purchased from Gordon's Specialty Stockfeeds (Yanderra, Australia). The diet contained the following macronutrient breakdown: 23% crude protein, 6% crude fat (21% saturated fat, 43.9% mono-unsaturated fat and 30.7% poly-unsaturated fat) and 5% crude fibre. This chow diet contains ingredients such as wheat, sorghum, soybean meal, pollard, bran, meat and bone meal, bloodmeal, fish meal, lucerne meal, vegetable oil, sunflower meal, salt, vitamin and mineral premix, amino acids and choline chloride. A total of 55 mice were used in this experiment; $n = 30$ male mice (15 MJD and15 non-transgenic littermates) and $n = 25$ female mice (13 MJD and 12 non-transgenic littermates). Experimental animals underwent repeated testing at different time points of the disease by an experimenter blinded to experimental groups.

2.2. Neurological monitoring

All mice underwent weekly behavioural and neurological monitoring during the light cycle. Neurological symptoms such as hind limb reflex, tremor and ataxic gate were scored on a four-point scale and the total score was recorded. For assessment of hind limb reflex, the animal was suspended by the tail and the splaying of the hind limbs was scored (score of 0 representing normal and score of 4 representing hindlimb paralysis). Tremor was scored from 0 (no tremor) to 4 (continuous pronounced tremor). Gait abnormalities were scored from normal gate (0) through to hindlimbs unable to be used for forward motion (4). Once animals reached a total neurological and behavioural score > 7, monitoring was increased to 2–3 times per week. Animals were weighed weekly during behaviour and neurological assessment. Animals were deemed to have reached humane endpoints upon reaching a total score of 10 and were euthanised via anaesthetic overdose (intraperitoneal injection of 300 mg/kg sodium pentobarbitone).

2.3. Summary of motor performance testing

Each mouse underwent a battery of motor performance tests including assessment of muscle strength testing (peak force exerted during grip strength and latency to fall from an inverted grid) and tests of balance and coordination (latency to cross a beam and latency to fall from an accelerating rotarod). Tests were performed once every 4–8 weeks to minimise confounding effects of repeated testing. All behavioural tests were conducted within the light phase (09:00–14:00).

2.4. Examination of muscle strength

For grip strength testing, mice were placed on plastic grid connected to a digital force metre (Model 47,200, Ugo Basile). Mice were allowed to grip onto the connected plastic grid with all four limbs, the maximal force (peak grams of force) emitted within a 20 s period was recorded. Mice underwent a minimum of 2 × 20 s trials. If trial scores differed by greater than 50gf, a third 20 s trial was performed. The average of all trials was recorded.

For inverted grid testing, mice were placed on a wire cage lid which was slowly inverted and held 50 cm above a soft, fabric landing zone. The time taken for mice to fall from the inverted grid was recorded (one trial performed per mouse). The maximum trial time was 60 s, after which mice were gently removed.

2.5. Examination of balance and coordination

Balance and coordination were examined by testing the amount of time required for each mouse to traverse a 12 mm wide square beam. The square beam was 1 m long and elevated 50 cm off the ground. A light was placed at the start of the beam and a dark box was placed at the end to encourage mice to traverse. Mice underwent three un-timed training sessions (three times per week, 5 weeks of age) to learn the task. Once mice had learnt the task and were able to traverse the beam in 10 s or less, they progressed to monthly timed trials (two timed trials per test session). The time taken to traverse the beam during test sessions was recorded and mice underwent a total of two test trials per test session. The average of the two test sessions was statistically analysed.

An accelerating rotarod was used to examine balance, coordination and stamina. Mice were placed on the accelerating rotarod apparatus (Model 7650, Ugo Basile) facing away from the experimenter, moving in the forward direction. Testing commenced at a speed of 4 rpm and increased to 40 rpm over 180 s. The total time taken to fall from the accelerating rotarod was recorded automatically and a maximum score of 300 s was recorded if mice did not fall from the rotarod. The apparatus was cleaned with F10 disinfectant between trials. Each animal underwent a single trial at each timepoint.

2.6. 16S rRNA amplicon sequencing of the faecal microbiota

Faecal samples were aseptically collected from 55 individual mice (30 male mice; 15 MJD/15 non-transgenic littermates and 25 female mice; 13 MJD/12 non-transgenic littermates) at three stages of the disease: early (week 7), symptomatic (week 11) and well-established (week 15) stages. Samples were stored at −80 °C prior to microbiota analyses. Total DNA was isolated from faecal samples using a FastDNA Spin kit (MP Biomedicals, Australia) according to the manufacturer's instructions. The V4 region of the 16S rRNA gene was amplified using 515F (5′-GTGCCAGCMGCCGCGGTAA-3′) and 806R (5′-GGACTACHVGGGTWTCTAAT-3′) primers with Golay barcodes and a Platinum™ Hot Start PCR master mix (Thermo Fisher Scientific, Australia). Resulting amplicons were quantified using a Quant-iT™ PicoGreen® dsDNA assay kit (Invitrogen, Australia) and equal molar amounts of barcoded amplicons from each sample were pooled prior to gel purifying the amplicons using a Wizard® SV gel and PCR cleanup system (Promega, Australia). Multiplexed amplicons were sequenced using an Illumina MiSeq (2 × 250 bp) platform at the Ramaciotti Centre for Genomics, Australia.

2.7. Bioinformatics and statistical analysis of sequence data

Raw sequence data was processed using Quantitative Insights Into Microbial Ecology software (QIIME2 version 2021.4) (Bolyen et al., 2019). Demultiplexed paired-end reads were quality filtered (median q < 30 and read length < 156 bp), followed by denoising with Deblur (Amir et al., 2017). Identified amplicon sequence variants (ASVs) were aligned with mafft (Katoh et al., 2002) which was used to construct a phylogenetic tree with FastTree2 (Price et al., 2010). ASVs were assigned to taxonomy at 99% similarity using the classify-sklearn naïve Bayes taxonomy classifier against the SILVA 138 database (Quast et al.,

2013) of the 515F/R806 region of the 16S rRNA gene. A total of 6,530,620 reads (mean 40,307 ± 9648) were obtained after quality filtering, each sample was rarefied at 21,700 reads prior to statistical analyses.

The ordination of the microbiota community structure was visualized using multidimensional scaling (MDS) plots. These were constructed based on Bray-Curtis similarity matrices of the abundance of ASVs using the vegan R package (Jari Oksanen et al., 2019). Statistical significance of observed differences in microbiota community structure between genotype and sex was determined using Permutational multivariate analysis of variance (PERMANOVA) tests with 9999 permutations. The alpha diversity was examined using the Shannon diversity index, Simpson's evenness index and richness expressed as the number of ASVs, all indices were determined using QIIME2.

Linear Discriminant Analysis effect size (LEfSe) method (online Galaxy Version 1.0) (Segata et al., 2011) was used to identify ASVs with significantly different ($p < 0.05$) abundances between genotypes and sexes at each of the three timepoints. MJD and WT or male and female were used as class of subjects with no subclasses. Linear Discriminant Analysis (LDA) score for each ASV was determined using default parameters: Kruskal-Wallis test among classes ($p < 0.05$), Wilcoxon test between classes ($p < 0.05$) and the threshold on logarithmetic LDA score for discriminative features >2.0. Multiple comparison adjustment was performed for all p values using Benjamini and Hochberg's false discovery rate (5%) correction. The abundance (Log_{10} transformed) of the ASVs that were found to be significantly different between groups were used to construct unpaired heatmaps using GraphPad Prism (version 9.5) software (GraphPad Software, La Jolla California, USA).

2.8. Correlation network analysis

Pair-wise correlations between the relative abundance of ASVs that had significantly different abundances between groups and behavioural data were examined using the Hmisc R package (Harrell, 2021). Bacterial ASVs and neurological data that showed significant differences between MJD and WT groups at each timepoint were used for correlation analysis. Statistically significant correlations ($p > 0.05$, FDR 5%) were used to generate correlation networks using Cytoscape sotfware (version 3.6.1).

2.9. Statistical analysis

Three-way repeated measures ANOVA (factor 1 sex, factor 2 genotype, repeated measures factor 3 age) was used to analyse weight progression. A mixed-effects model (REML) with factors of sex and genotype and a repeated measure of time was used to analyse total neurological scores. Unpaired *t*-tests were used to compare the number of inherited CAG repeats and survival (total number of days) across MJD male and female animals. A log-rank (Mantel-Cox) test was used to compare Kaplan meier survival curves. Two-way ANOVAs (factor 1 genotype, factor 2 age) were used to analyse motor behavioural data (beam test, grip strength, inverted grid and accelerating rotarod) across different timepoints in disease progression. Mixed-effect analysis with Sidak's multiple comparisons tests were used to examine the statistical significance of the differences in Shannon diversity indices and *Firmicutes/Bacteroidota* ratios between groups.

3. Results

3.1. Male and female MJD mice develop disease phenotypes at different rates

First, we examined the presence of phenotypic differences between male and female mice expressing human mutant *ATXN3* (MJD) compared to non-transgenic (wild-type, WT) littermate controls. Analysis of weight progression revealed significant main effects of sex ($p < 0.0001$), genotype ($p < 0.0001$) and age ($p < 0.0001$). We also detected significant interaction effects; sex x age $p < 0.0001$, genotype x age $p < 0.0001$, and sex x genotype x age $p < 0.0001$. Male and female WT mice continue to gain weight throughout their lifetime, whilst male and female MJD remain at a stable weight from around 8 weeks of age (Fig. 1B). Weekly neurological assessments revealed the presence of neurological symptoms from as early as 8 weeks of age in MJD animals, as indicated by increased total neurological score (Fig. 1C). Analysis of the neurological score data revealed significant main effects of genotype ($p < 0.0001$) and age ($p < 0.0001$). Analysis of neurological score also revealed statistically significant interaction effects; sex x age $p < 0.0017$, genotype x age $p < 0.0001$ and sex x genotype x age $p < 0.0141$. Similar to MJD patients, neurological symptoms progressively worsen with age in MJD mice, producing severe neurological impairments towards the end of life. Transgenic CMVMJD135 mice were also found to display decreased survival, with MJD males and MJD females reaching humane endpoints prior to 170 days of age and 190 days of age, respectively (Fig. 1D). Comparison of survival curves using the Log-rank (Mantel-Cox) test revealed a significant difference in survival across compared groups ($X^2 = 31.56$, df = 3, $p < 0.0001$). MJD animals displayed decreased survival compared to WT littermates, as expected. Interestingly, MJD males also displayed decreased survival when compared with MJD females ($p < 0.0001$), with MJD females surviving approximately 20 days longer than MJD males. This striking effect of sex on survival has not been reported in previous studies describing the survival of CMVMJD135 mice. To confirm that the differences observed in neurological score and survival across male and female MJD mice were not due to differences in the inherited CAG repeat, we compared the CAG repeat expansion length across male and female MJD mice. There was no significant difference between the CAG repeat length detected in male and female MJD mice ($p = 0.7386$, Fig. 1E).

Next, we examined the effect of mutant *ATXN3* expression on motor behaviours. Due to the sex differences detected in survival, motor performance of male and female mice was analysed separately. The time taken to traverse the balance beam was used as a test of balance. In male mice, we detected a significant main effect of genotype ($p < 0.0001$) and age ($p < 0.0001$). Further, we also detected a significant genotype x age interaction effect ($p < 0.0001$), whereby MJD males took significantly longer to cross the beam as age increased (Fig. 1F). Statistically significant differences in the ability to cross the balance beam were detected across genotypes at the three tested time points, 14 weeks of age ($p = 0.0014$), 18 weeks of age ($p = 0.0003$) and 22 weeks of age ($p = 0.0256$). Two motor tests were used examine muscle strength: grip strength and inverted grid tests. We detected a significant effect of genotype ($p = 0.0358$) and age ($p < 0.0001$) on grip strength performance (Fig. 1G) whereby MJD males exerted less peak force than WT males, with post hoc comparisons revealing a significant difference across genotypes at 15 weeks of age ($p = 0.0208$). Analysis of inverted grid performance revealed a significant effect of genotype and age ($p = 0.0032$ and $p = 0.0138$, respectively, Fig. 1H). Post-hoc multiple comparisons revealed a statistically significant difference between WT and MJD males at 10 weeks of age ($p = 0.0032$), whereby MJD males took a shorter time to fall from the inverted grid apparatus. Lastly, performance on an accelerating rotarod was used to measure motor performance and coordination. We detected a significant effect of genotype ($p = 0.0195$) and a genotype x age interaction effect ($p = 0.0169$) on rotarod performance, where MJD males took a significantly shorter time to fall from the rotarod as age increased. Post hoc multiple comparisons revealed a statistically significant difference between MJD male and WT male rotarod performance at 13 and 17 weeks of age ($p = 0.0217$ and $p = 0.0092$, respectively, Fig. 1I).

Female mice were exposed to the same battery of motor tests. First, we detected a significant main effect of genotype ($p < 0.0001$) and age ($p < 0.0001$) on balance beam performance whereby MJD females took longer to traverse the balance beam than WT females. Post-hoc comparisons revealed that WT females were able to cross the balance beam

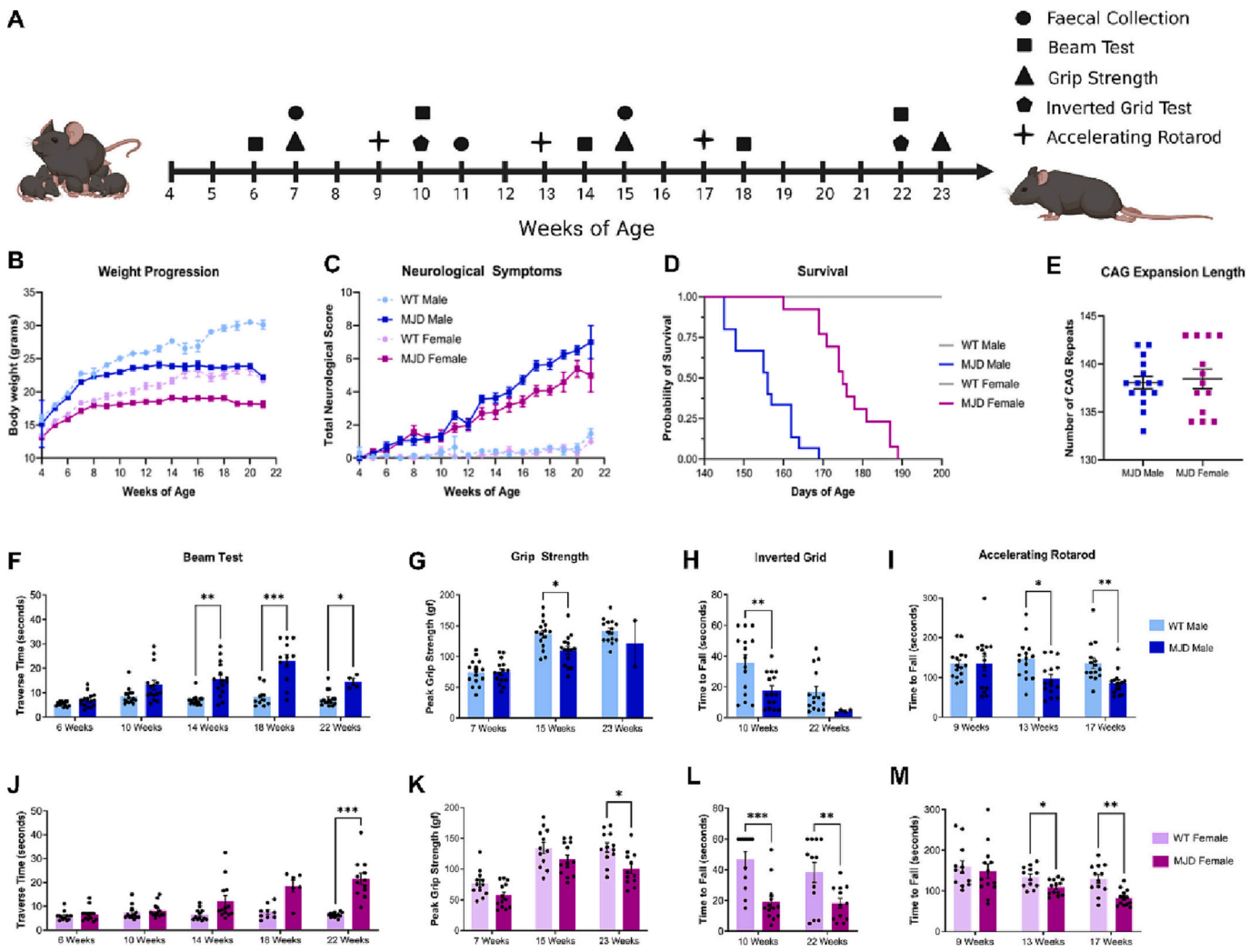

Fig. 1. Male and female mice expressing mutant human *ATXN3* to model MJD develop neurological and motor impairments that progressively worsen with age. (A) A schematic of the study design, including collection of faecal samples and motor behaviour testing at the ages indicated. A total of 55 mice were used: $n = 30$ male (15 MJD and 15 non-transgenic WT littermates) and $n = 25$ female (13 MJD and 12 non-transgenic WT littermates). Timeline figure was created using BioRender.com. **(B)** Male and female MJD mice do not continue to gain weight throughout life like wild-type littermate controls, instead weight gain stagnates from neurological symptom onset. **(C)** MJD mice develop neurological symptoms (abnormal hindlimb reflex, tremor and gait abnormalities) which progressively worsen from 10 weeks of age, as indicated by an increased total neurological score compared to wild-type siblings. **(D)** MJD mice display decreased survival when compared to wild-type siblings, with male MJD mice displaying shorter survival when compared to female MJD mice. **(E)** Comparison of the inherited CAG repeat length of male and female MJD mice revealed no statistical difference between the groups. Within the male mice, a range of differences was found between the MJD and WT littermates within the **(F)** balance beam test; **(G)** grip strength test; **(H)** inverted grid test; and **(I)** accelerating rotarod test. Female MJD mice were found to develop motor phenotypes at later ages with statistically significant genotype differences detected for the **(J)** balance beam; **(K)** grip strength testing; **(L)** inverted grid muscle strength testing; and **(M)** accelerating rotarod. All data is presented as group mean ± SEM, $n = 12$–15 per group. * Represents $p < 0.05$, ** represents $p < 0.01$ and *** represents $p < 0.001$.

significantly faster than MJD females at 18 weeks ($p = 0.0295$) and 22 weeks of age ($p = 0.0002$, Fig. 1J). Further, we also detected a significant genotype x age interaction effect ($p < 0.0001$) on balance beam performance, suggesting that balance impairments worsened with age in MJD females. Examination of muscle strength via grip strength performance revealed a significant effect of both genotype ($p = 0.0001$) and age ($p < 0.0001$). Post-hoc comparisons revealed significant difference between genotypes at 23 weeks of age ($p = 0.0123$, Fig. 1K), again suggesting that MJD females displayed reduced muscle strength than WT females. Further analysis of muscle strength via inverted grid testing revealed a significant effect of genotype on test performance ($p = 0.0002$). Multiple comparisons revealed a statistically significant difference between WT females and MJD females at 10 weeks of age ($p = 0.0003$) and 22 weeks of age ($p = 0.0093$, Fig. 1L). Interestingly, we detected a genotype effect in inverted grid performance at a much earlier age (10 weeks of age) than grip strength performance (genotype effect first detected at 23 weeks of age) in females. We hypothesise that this may because the inverted grid test might be more challenging, as animals must hold their body weight against gravity whereas the grip strength testing is performed vertically and thus not as challenging. Lastly, we detected a significant main effect of both genotype ($p = 0.0204$) and age ($p = 0.0005$) on rotarod performance. Multiple comparisons revealed a significant difference between genotypes at 13 weeks of age ($p = 0.0347$) and 17 weeks of age ($p = 0.0035$, Fig. 1M), suggesting MJD females displayed impaired motor coordination compared to WT females. Interestingly, female MJD mice developed motor impairment at later ages on two tests, with a significant effect of genotype first detected at 22 weeks of age for balance beam (detected from 14 weeks in male MJD mice) and at 23 weeks of age for grip strength (first detected at 15 weeks in MJD males).

3.2. MJD mice had an altered overall gut microbiota community structure

Faecal samples collected at 7, 11 and 15 weeks of age were used to examine the gut microbiota through sequencing of the 16S rRNA gene amplicons. The microbiota community structure of MJD mice was significantly different compared to that of WT mice (Fig. 2), where male and female transgenic mice had clear shifts in the microbial community structure compared to WT mice at all three time points. While shifts of the microbiota community structure in male MJD mice were not statistically significant at 7 weeks ($p = 0.06$, PERMANOVA, Fig. 2A), these became distinct by week 11 ($p = 0.02$), which got more pronounced at week 15 ($p = 0.0001$) resulting in significantly divergent microbiota structures in MJD males compared to that of WT males. Female MJD mice demonstrated significant differences in microbiota structure at 7 weeks of age ($p = 0.02$, Fig. 2B), these were maintained at weeks 11 and 15 ($p = 0.03$ and $p = 0.01$, respectively) without a substantial increase in microbiota community shifts over time, unlike the highly divergent microbiota communities observed in male MJD and WT mice.

The diversity of the microbiota community was examined using three alpha diversity indices: Shannon diversity index, Simpson's evenness index and richness expressed as the number of amplicon sequence variants (ASVs) identified in each sample (Fig. S1A-F). Male MJD and WT mice demonstrated no significant differences in all three microbiota diversity indices at the three tested time points. Whilst there were significant differences in microbiota diversity of female MJD mice at 7 weeks of age, no significant differences at 11 and 15 weeks of age were observed. Where MJD females had a lower microbiota diversity ($p = 0.02$, Fig. S1B) with a higher number of ASVs ($p = 0.04$, Fig. S1F) at 7 weeks compared to WT female mice, there were no statistically significant differences in Simpson's evenness indices of female mice at week 7.

3.3. The gut microbiota composition of MJD mice was different at all three time points

The microbiota of both MJD and WT mice was dominated by the bacterial phyla *Bacteroidota*, *Firmicutes* and *Verrucomicrobiota* (Fig. S1G). The exact abundance of all phyla differed between mice depending on the genotype, age and sex. Upon comparison of the ratio between the abundance of *Firmicutes* and *Bacteroidota*, no significant differences were observed at 7, 11 or 15 weeks between MJD and WT in both male and female mice (Fig. S1H–I).

At the bacterial family level, the microbiota of all mice was mainly composed of *Muribaculaceae, Akkermansiaceae* and *Lachnospiraceae* families (Fig. 2C), but there were significant differences in their abundance between MJD and WT, and between male and female mice. For example, the relative abundance of *Akkermansiaceae* was lower in male MJD mice at 11 ($p = 0.0036$) and 15 ($p = 0.01$) weeks of age compared to WT males, while the same family had a higher abundance in female MJD mice at week 11 compared to WT females ($p = 0.0001$). Further, the abundance of *Muribaculaceae* was higher in MJD males than WT

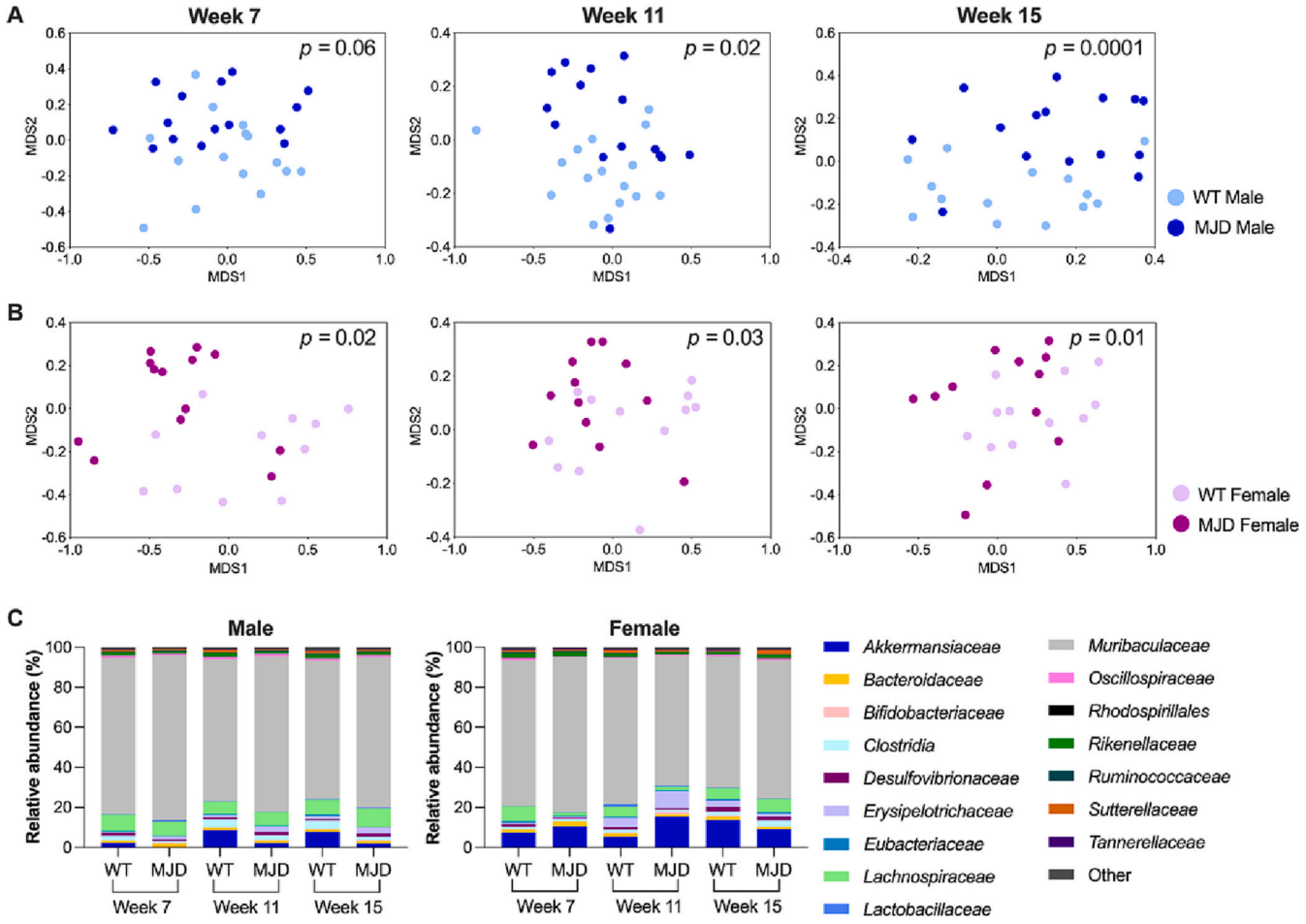

Fig. 2. Overall community structure and composition of the gut microbiota of MJD and WT littermate mice at three different ages. The ordination of the microbiota community was visualized using Bray-Curtis similarity-based MDS plots and the statistical significance of differences was determined using PERMANOVA. Microbiota community structure of **(A)** male and **(B)** female mice of the CMVMJD135 (MJD) transgenic mouse line and littermate controls (WT) are shown for weeks 7, 11 and 15. **(C)** Family level taxonomic composition of the gut microbiota samples collected from male and female MJD and WT mice at weeks 7, 11 and 15. The relative abundance (%) for each family is shown, bacterial families with a relative abundance <1% in all samples are categorised as "Other".

males at 11 ($p = 0.0012$) and 15 ($p = 0.0075$) weeks of age, while the relative abundance of this family was lower in MJD female mice at week 11 compared to that of WT females ($p = 0.0004$). The abundance of *Lachnospiraceae* in MJD females was lower at week 7 compared to that of WT females ($p = 0.039$), while no statistically significant change was observed in MJD males compared to WT males.

The abundance of microbial species equivalents, demonstrated as ASVs, was examined using LEfSe analysis to identify distinct ASVs between MJD and WT mice, separate analyses were performed for sex and the three tested ages. The abundance of several ASVs was significantly different in the gut microbiota of MJD mice compared to WT mice at week 7 (Fig. 3), week 11 (Fig. S2) and week 15 (Fig. S3). Some of these differences occurred even before the onset of MJD symptoms, whereby male MJD (Fig. 3A) and female MJD (Fig. 3B) mice had 66 and 60 differentially abundant ASVs, respectively, at 7 weeks of age compared to their respective WT groups. By week 11 (Fig. S2A) and 15 (Fig. S3A), the relative abundance of 75 and 110 ASVs, respectively, were significantly different in male MJD mice compared to male WT mice. Whilst 62 and 57 ASVs had different abundances in female MJD mice compared to female WT mice at week 11 (Fig. S2B) and 15 (Fig. S3B), respectively. In addition to demonstrating changes in the abundance of a larger number of ASVs in male MJD mice compared to that of female MJD mice, this data indicates that a greater proportion of ASVs having a higher abundance in MJD males at 7 (41%) and 11 (44%) weeks of age compared to that of MJD females at 7 (13%) and 11 (19%) weeks.

Many ASVs in the families *Lachnospiraceae, Muribaculaceae, Oscillospiraceae,* and *Ruminococcaceae* and order *Clostridia* had different abundances in MJD mice. Some of the ASVs were differentially abundant in MJD mice consistently at all three tested ages. For example, male MJD mice had a lower abundance of ASVs in the families *Lachnospiraceae* (ASV158 and 343), *Muribaculaceae* (ASV40 and 11), *Rikenellaceae* (ASV56 and 49) and *Oscillospiraceae* (ASV109) at 7, 11 and 15 weeks of age, whilst the abundance of ASVs in *Lachnospiraceae* (ASV554, 300, 328 and 145), *Bacteroidaceae* (ASV284) and *Bifidobacteriaceae* (ASV7) families was higher compared to that of WT males (Table S1). In female MJD mice, ASVs in *Muribaculaceae* (ASV11 and 631), *Rikenellaceae* (ASV56), *Bacteroidaceae* (ASV430), *Rikenellaceae* (ASV446) and *Lachnospiraceae* (ASV137) were lower in abundance at weeks 7, 11 and 15, whereas the abundance of *Clostridia* (ASV50) and *Rikenellaceae* (ASV9) was higher (Table S2). In addition to these changes that were consistently observed across all three tested ages, most alterations to microbiota composition were specific to each stage of MJD development. Many of these disease state-specific changes were seen in ASVs belonging to the families *Lachnospiraceae, Muribaculaceae, Oscillospiraceae,* and *Ruminococcaceae*

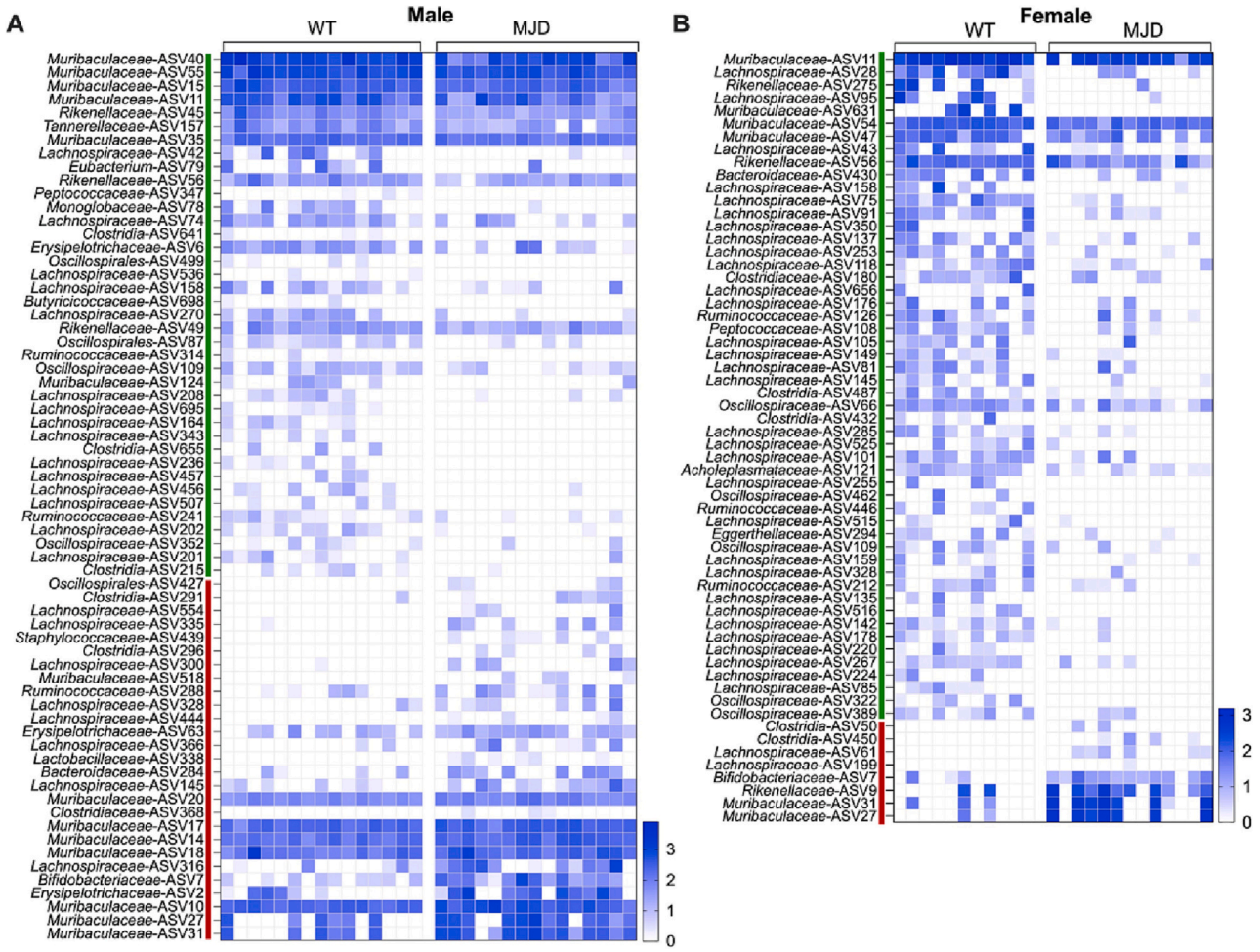

Fig. 3. Pre-symptomatic (week 7) MJD mice had significantly different amplicon sequence variant (ASV) abundances compared to the WT mice. Distinct ASVs between MJD and WT groups were identified using the linear discriminant analysis effect size (LEfSe) method. The set of ASVs found to be differentially abundant in the MJD group are shown for **(A)** male and **(B)** female mice. The unpaired heatmaps show the relative abundance (Log_{10} transformed) of the ASVs, rows correspond to the ASVs, and columns correspond to individual mice in each genotype. Blue and white denote the highest and lowest relative abundance, respectively, as shown in the legend. ASVs with significantly higher and lower abundances in the MJD group compared to the WT mice are indicated by a red and green line, respectively. The abundance of each ASV in male and female mice is provided in Table S1 and Table S2. (For interpretation of the references to colour in this figure legend, the reader is referred to the web version of this article.)

and order *Clostridia* (Fig. 3, Fig. S2 and Fig. S3).

3.4. Male and female mice had different gut microbiota alterations with MJD

How the gut microbiota of male and female mice changed with the development of MJD was examined through comparing the microbiota community structure and composition of male and female mice at 7, 11 and 15 weeks of age. There were greater differences in microbiota community structure between male MJD and female MJD mice at all three time points ($p < 0.0008$, PERMANOVA, Fig. 4A) compared to that between male WT and female WT mice ($p < 0.04$, Fig. 4B). LEfSe analyses were used to identify distinct ASVs between male and female MJD mice and male and female WT mice at each week (Table S3). The set of ASVs that had different abundances in male MJD mice compared to female MJD mice was substantially different from that of WT male and female mice. Of the 103 ASVs that had different abundances between male and female MJD mice at week 7, 89 ASVs were uniquely different in MJD mice compared to the set of ASVs that was different between WT male and female mice. These uniquely different ASVs in MJD males compared to MJD females were in the families including *Lachnospiraceae* and *Muribaculaceae* and order *Clostridia.* Similarly, at weeks 11 and 15, a unique set of 77 (out of 86) and 78 (out of 85) ASVs, respectively, were different between male and female MJD mice.

To identify sex-specific gut microbiota changes with the development of MJD, the ASVs found to have significantly different abundances between MJD and WT mice in either sex at week 7 (Fig. 3), week 11 (Fig. S2) and week 15 (Fig. S3) were examined. Despite having some specific ASVs that changed similarly in male and female mice with the development of MJD, most of the ASVs that were differentially abundant with MJD were sex-specific. For example, at week 7, except for 9 ASVs that were consistently different in the microbiota of male and female MJD mice compared to their respective WT groups, all other ASV changes were unique to each sex. Similarly, at weeks 11 and 15, there were only 18 and 15 ASVs, respectively, that were consistently different in both male and female MJD mice. However, at the bacterial family level, there were similarities in MJD-associated microbiota changes between the sexes, where both male and female MJD mice had differences in the abundance of *Lachnospiraceae, Muribaculaceae, Ruminococcaceae* and *Oscillospiraceae* compared to the WT groups.

3.5. Microbiota changes at week 7 correlated with symptoms in well-established disease state

To examine how gut microbiota changes observed in MJD mice at the pre-symptomatic state associate with the development of symptoms, pairwise correlation analyses were conducted between the abundance of ASVs that were significantly different in MJD mice at week 7 and their behaviour after symptom onset (14–17 weeks of age). Separate networks were constructed for male (Fig. 5A) and female (Fig. 5B) animals, both of which showed significant correlations between the abundance of ASVs at week 7 and symptoms at later stages of the disease. In both male and female mice, the abundance of some ASVs in the families *Lachnospiraceae, Oscillospiraceae* and *Rikenellaceae* showed positive correlations with accelerating rotarod and grip strength, while they were negatively correlated with the neurological score and balance beam data. This observation suggests that these ASVs are associated with motor and neurological impairment; mice with a lower abundance of these ASVs spent less time on the rotarod before falling and had a lower grip strength, whilst taking longer to cross the balance beam and had higher neurological scores (indicated greater impairment). Similarly, some ASVs in the family *Muribaculaceae* showed positive correlations with accelerating rotarod, while having a negative correlation with the neurological score, suggesting that a lower abundance of those ASVs was correlated with shorter times on the rotarod and greater neurological impairment. Other ASVs in the same family showed different associations with the symptoms, where they showed positive correlations with the neurological score, balance beam and accelerating rotarod and showed negative correlations with grip strength.

Given the delay in the onset of symptoms in female animals (Fig. 1), we examined the association of the microbiota changes in female MJD mice at week 7 with their behaviour at the advanced state of the disease (20–23 weeks of age, Fig. S4). Compared to the correlations between the microbiota of female mice at 7 weeks and their behaviour at week 15 (Fig. 5B), there were stronger and a greater number of statistically significant correlations between week 7 microbiota and behaviour at 20–23 weeks of age (Fig. S4). For example, ASVs in *Lachnospiraceae, Oscillospiraceae* and *Rikenellaceae* were positively correlated with accelerated rotarod, grip strength and inverted grid test results, while they negatively correlated with the neurological score and beam test results.

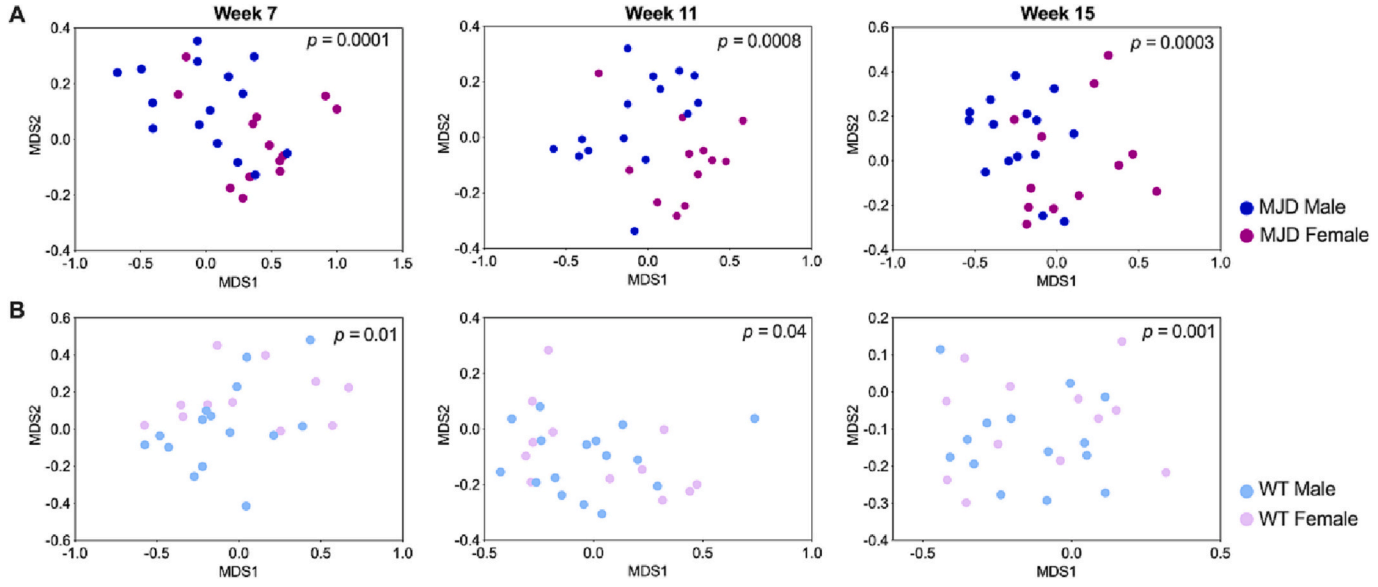

Fig. 4. Ordination of the gut microbiota community structure of male and female MJD and WT mice at weeks 7, 11 and 15. MDS plots were constructed using Bray-Curtis similarity of the ASV abundance and the statistical significance of differences was determined using PERMANOVA analyses. Microbiota community structure of **(A)** male vs female MJD mice and **(B)** male vs female WT mice are shown for weeks 7, 11 and 15.

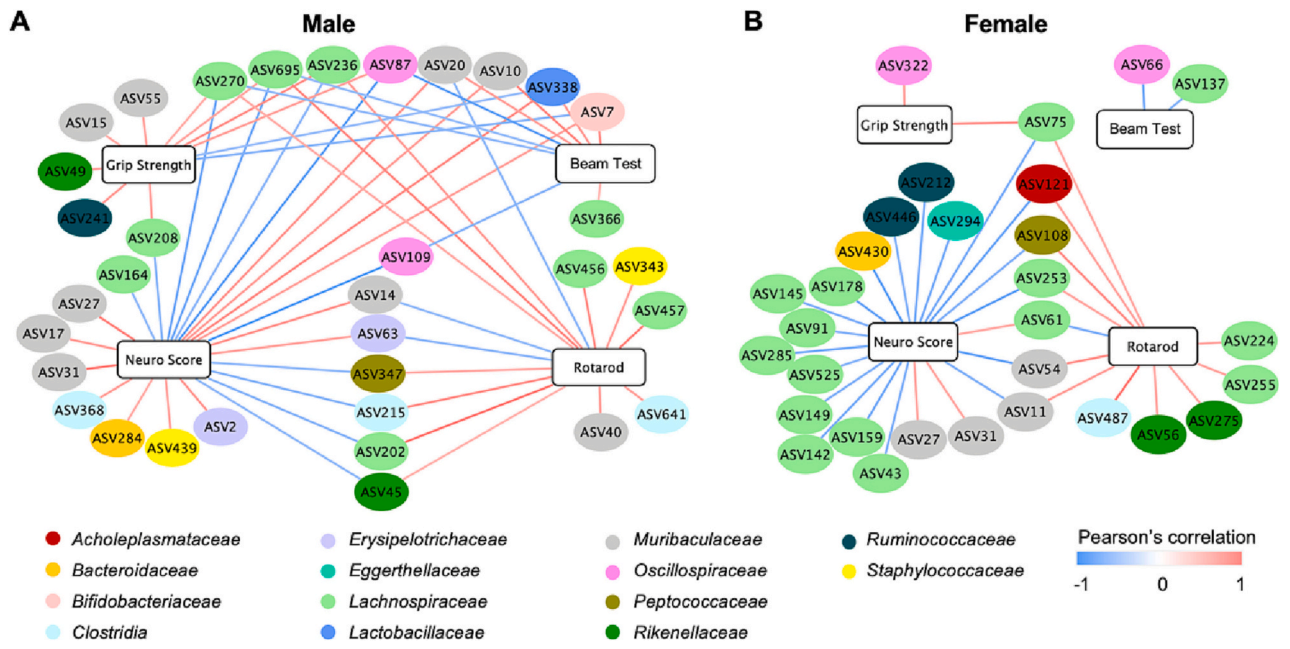

Fig. 5. Networks showing how the microbiota changes at a pre-symptomatic age (week 7) correlated with the severity of symptoms at later disease stages (week 14–17). Using pairwise correlation analysis, the associations between differentially abundant amplicon sequence variants (ASVs) in MJD mice at week 7 and behaviour and neurological data were identified, and significant correlations ($p < 0.05$) were used to construct networks. Data show how pre-symptomatic changes in microbial ASVs in **(A)** male and **(B)** female MJD mice correlated with neurological (Neuro) score, grip strength, accelerating rotarod and beam tests. The ASVs are shown in colour-coded dots based on the taxonomic assignment at the family level. A positive or negative Pearson correlation coefficient is presented by a red or blue line, respectively, the intensity of the colour denotes the strength of the correlation. (For interpretation of the references to colour in this figure legend, the reader is referred to the web version of this article.)

We then examined how the abundance of microbes that showed strong correlations with MJD symptoms changed over time (Fig. 6A and B). Firstly, ASVs that were different between MJD and WT mice consistently at 7, 11 and 15 weeks were identified. Compared to WT males, 17 ASVs were differentially abundant in MJD males across all three timepoints (Table S1D), whilst 8 ASVs had different abundances in MJD females compared to WT females consistently at weeks 7, 11 and 15 (Table S2D). These ASVs mainly belonged to the families *Muribaculaceae* and *Rikenellaceae, Lachnospiraceae* mice. Upon examination of how these microbes correlated with motor deficits observed at weeks 15–23 (Fig. 5 and Fig. S4), 6 and 5 ASVs in male and female mice, respectively, were found to have strong links (Fig. 6). The abundance of some of these ASVs remained similar in MJD mice across weeks 7, 11 and 15, while others (ASV 40, 7, 56 and 137) continued to change with the development of MJD at 11 and 15 weeks, demonstrating a diverging shift in their abundance between MJD and WT mice.

Correlation network analyses between the microbiota of MJD mice at week 7 and the age of disease onset and survival revealed significant associations in both male (Fig. S5A) and female (Fig. S5B) MJD mice. The abundance of specific ASVs in the *Lachnospiraceae* family positively correlated with survival and age of MJD onset, indicating that a lower abundance of members in *Lachnospiraceae* may link with the early onset

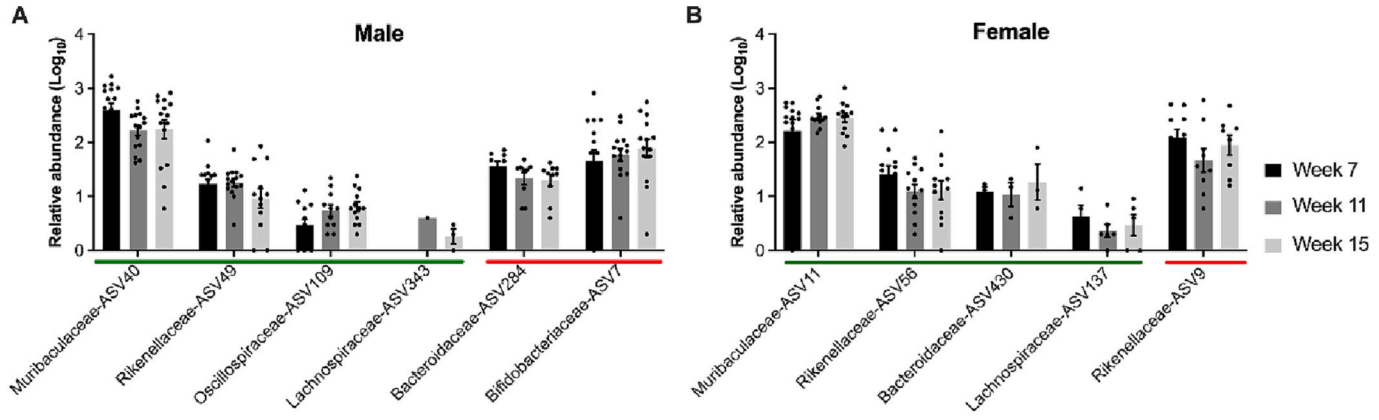

Fig. 6. The abundance of amplicon sequence variants (ASVs) that showed strong correlations with symptoms and were differently abundant in MJD mice at all disease stages (weeks 7, 11 and 15). The linear discriminant analysis effect size (LEfSe) method was used to identify ASVs that had significantly different abundances in MJD mice at weeks 7, 11 and 15 compared to WT mice. ASVs that were consistently different between MJD and WT mice at all three time points and correlated with symptoms at the well-established or advanced state were identified. The relative abundance (Log_{10} transformed, mean ± SD) of these ASVs at weeks 7, 11 and 15 is shown for **(A)** male and **(B)** female MJD mice. ASVs with significantly higher and lower abundances in the MJD group compared to the WT mice are indicated by a red and green line, respectively. (For interpretation of the references to colour in this figure legend, the reader is referred to the web version of this article.)

of symptoms and reduced lifespan. While some correlations were similarly observed in both male and female MJD mice, most were sex-specific. For example, the abundance of ASVs in *Ruminococcaceae* and order *Clostridia* positively correlated with survival in MJD males, whilst a different set of ASVs in *Ruminococcaceae* and *Clostridia* negatively correlated with survival in MJD females.

4. Discussion

4.1. MJD-associated alterations in the gut microbiota initiated before the onset of symptoms

Our study demonstrates for the first time that the neurodegenerative disease MJD is associated with changes in the gut microbiota community structure and composition. These microbiota alterations were seen as early as 7 and 11 weeks of age (Fig. 2 and Fig. 3), prior to detection of any motor impairments in the transgenic mice (Fig. 1). This suggests that the gut microbiota may change prior to the onset of neurological symptoms in MJD. Similar to our observations, previous gut microbiota studies on other neurogenerative diseases, including MND (Blacher et al., 2019), Alzheimer's disease (Vogt et al., 2017) and Parkinson's disease (Scheperjans et al., 2015) have demonstrated clear shifts in the gut microbiota of mouse models and patients with these conditions compared to healthy controls. In fact, the onset of some neurodegenerative conditions, such as MND and Parkinson's disease, have been linked with early changes in the functions and microbial communities in the gut before neurological symptoms appear. For example, it has been found that people with Parkinson's disease have a lower abundance of the *Prevotellaceae* in their gut microbiomes (Scheperjans et al., 2015), while most patients experience intestinal issues, including constipation before the onset of any neurological symptoms (Adams-Carr et al., 2016; Savica et al., 2009). Our mouse model data demonstrates that MJD is also associated with microbiota changes that occur before any known symptoms of MJD are detected. This may indicate that microbiota changes are one of the first symptoms to appear and may even play a role in the development of symptoms that have been historically described with MJD. There is existing evidence to suggest autonomic dysfunction, due to degeneration of nuclei responsible for autonomic functions (Rüb et al., 2003; Shimizu et al., 2010), is present in MJD patient cohorts and that gastrointestinal issues, such as constipation and diarrhea can occur at different stages of disease development (França Jr et al., 2010; Yeh et al., 2005). Examining when dysbiosis in the gut microbiota first emerges and whether changes in intestinal functions and morphology occur with MJD will be useful extensions. These will help further understand the role of the gut in MJD development and how and when gut microbiota manipulation potentially impacts MJD onset and/or progression.

Microbiota alpha diversity was not significantly different between genotypes or ages, except for female MJD mice who had lower microbial diversities compared to WT females at 7 weeks of age (Fig. S1). This difference in alpha diversity was not observed at later stages of the disease or in male MJD mice at any of the three tested ages, including at 7 weeks. While our findings suggest no link between microbial alpha diversity and MJD development, this differs from previous work. For example, Blacher et al. (2019) reported increased microbiota alpha diversity in transgenic SOD1 mice modelling MND, and Kong et al. (2020) showed no significant differences in microbiota diversity in female Huntington's disease mice but increased microbiota diversity in male Huntington's disease mice at 12 weeks of age. Studies in patients have reported a lower microbial diversity in neurodegenerative conditions such as Alzheimer's disease (Vogt et al., 2017; Zhuang et al., 2018) and MND (Rowin et al., 2017). Overall, these observations indicate clear differences in how microbiota alpha diversity changes with neurodegeneration in different disease models, sexes, and organisms. Further studies will be necessary to understand the link between microbiota alpha diversity and neurodegeneration, particularly to identify the factors contributing to the discrepancies between studies.

4.2. Gut microbiota shifts increased with the development of MJD in a sex-specific manner

The gut microbiota community structure (Fig. 2) and composition (Fig. S2 and S3) of MJD mice shifted further from that of the WT group at 11 and 15 weeks, an age at which both male and female animals demonstrated MJD symptoms (Fig. 1). While some bacterial ASV abundances were consistently different in MJD mice at 7, 11 and 15 weeks of age, most MJD-associated microbiota composition changes were specific to one disease stage. Further studies using techniques such as metagenomics and metabolomics to examine the functional potential of these microorganisms and targeted examinations on culture isolates of these bacteria will be necessary to elucidate whether these disease state-specific compositional changes in the microbiota are linked to any functional changes in the microbial communities, gut functions and morphology and neurodegeneration.

Our data demonstrate sex-specific changes in the gut microbiota with MJD development. For example, while both male and female MJD mice had distinct microbiota community structures and compositions at week 7, these changes became more pronounced rapidly in male MJD mice, producing greater differences with higher statistical significance at 11 and 15 weeks compared to that of female MJD mice (Fig. 2, Fig. S2 and Fig. S3). Male MJD mice also demonstrated rapidly progressing motor deficits compared to female MJD mice (Fig. 1), conflicting with evidence from clinical MJD cohorts which suggest biological sex has no effect on disease onset, progression or overall survival (Kieling et al., 2007; Klockgether et al., 1998). Taken together, these observations propose that the extent of gut microbiota changes could impact the severity of MJD symptoms and progression. Furthermore, the exact nature of how the gut microbiota changed with the development of MJD was different between male and female mice, this was observed in addition to the sex-dependent microbiota variations observed in WT mice (Fig. 4 and Table S3).

In line with the sex-specific variations in the overall microbiota changes and disease development, we observed a lower abundance of the *Akkermansiaceae* family only in male MJD compared to WT male mice (Fig. 2C). In contrast, female mice had a higher abundance of this family compared to male mice, and female MJD mice in fact had a higher abundance of *Akkermansiaceae* compared to female WT. *Akkermansiaceae*, a bacterial family with members known to synthesis and/or catabolise tryptophan (Yang et al., 2020), has been reported to be present in higher abundance in individuals with milder progression of neurodegeneration (Cox et al., 2021) and increased longevity (Biagi et al., 2016) Tryptophan when catabolised by gut microbes, including *Akkermansiaceae,* produce several metabolites such as indole, indole derivatives and tryptamine that can regulate disease development associated with the central nervous system (Rothhammer et al., 2018), and may have a role in neuroprotection (Rothhammer et al., 2016). Furthermore, tryptophan is a precursor of serotonin, and modulation of serotonin signalling has been shown to decrease ataxin-3 aggregation in models of MJD (Teixeira-Castro et al., 2015). Speculatively, the lower abundance of *Akkermansiaceae* may be linked with decreased levels of tryptophan, associated metabolites and serotonin, therefore, leading to higher ataxin-3 aggregation and MJD progression. Direct experimental examination will be essential to confirm this potential link.

Additional sex-dependent differences in the microbiota at a family level included an increased abundance of *Muribaculaceae* in male MJD mice compared to WT controls at 11 and 15 weeks, while the abundance of *Lachnospiraceae* and *Muribaculaceae* was lower in female MJD mice at 7 and 11 weeks of age, respectively. The *Muribaculaceae* family is known to digest carbohydrates and has been proposed to play a role in regulating energy metabolism (Wang et al., 2020). Interestingly, *Lachnospiraceae* is a main producer of short chain fatty acids (SCFAs) such as acetate, propionate and butyrate through the digestion of dietary fibre

(Canani et al., 2011). Butyrate has received substantial attention in the literature as it has been demonstrated to have neuroprotective effects in cellular and animal model studies for a range of neurodegenerative diseases (Chou et al., 2011; Liu et al., 2017b; Qiao et al., 2020; Watchon et al., 2021; Zhang et al., 2022). Further, butyrate has been found to be at lower concentrations in the feces of mice and people with Parkinson's disease (Aho et al., 2021), Alzheimer's disease (Zhuang et al., 2018) and MND (Nicholson et al., 2021), suggesting that it may be decreased in MJD and has a role in disease development.

Overall, we observed clear sex-specific differences in the progression of neurological symptoms, motor deficits and gut microbiota changes related to MJD. A study of a mouse model of Huntington's disease reported significant differences between male and female gut microbiota, bodyweight, and faecal output (Kong et al., 2020). However, that study examined the microbiota at only one time point at the symptomatic stage. Our study shows that sex-dependent differences in the gut microbiota start early, relative to symptom development, and might contribute to disease progression. These sex-specific differences may be linked with the neuroprotective or mechanistic effects of sex hormones (Jurado-Coronel et al., 2018; Vegeto et al., 2019). As sex hormones are known to influence the composition of the gut microbiome (He et al., 2021; Valeri and Endres, 2021), it is plausible that sex hormones may also modulate gut-brain axis activity and the transmission of neurotoxic or neuroprotective metabolites from the gut to the central nervous system, and thus may directly or indirectly affect MJD pathogenesis. Future studies designed to understand the role of sex hormones in MJD development and gut microbiota alterations will be essential in confirming this. Furthermore, analyses of the gut microbiota functional differences between male and female mice will help determine the relevance of sex-specific gut microbiota differences in MJD pathogenesis.

4.3. Early gut microbiota changes correlated with the severity of symptoms at the well-established disease state

Microbiota changes at 7 weeks of age showed strong correlations with the severity of symptoms at the well-established (at 15 weeks) and advanced (at 20–23 weeks) state of MJD (Fig. 5 and Fig. S4). Particularly, ASVs in *Lachnospiraceae*, *Oscillospiraceae*, *Rikenellaceae* and some *Muribaculaceae*, which were lower in abundance in the microbiota of both male and female MJD mice at week 7 (Fig. 3), showed positive correlations with accelerating rotarod, grip strength and inverted grid performance later in the disease, while they showed negative correlations with neurological score and balance beam test. Overall, the severity of MJD symptoms was higher when the microbiota in the pre-symptomatic state had a lower abundance of specific ASVs in *Lachnospiraceae*, *Oscillospiraceae*, *Rikenellaceae*, *Muribaculaceae* and *Ruminococcaceae* (Fig. 3, Fig. 5, and Fig. S4). This may suggest a role of these microorganisms in MJD development. However, additional correlations were also found indicating that other ASVs, such as additional specific ASVs of *Muribaculaceae* were correlated in the reverse manner where a higher abundance of these ASVs was correlated with more severe disease phenotypes. These correlations need biological validation using targeted examinations, for example, supplementing with individual culture isolates and investigating the impact on MJD to confirm how they impact disease development.

Similar to our observations in MJD, a lower abundance of *Lachnospiraceae*, *Ruminococcaceae, Oscillospiraceae* and *Rikenellaceae* has been reported in patients and mouse models of Parkinson's disease (Cosma-Grigorov et al., 2020; Sampson et al., 2016), MND (Fang et al., 2016) and Huntington's disease (Wasser et al., 2020). Along with the *Lachnospiraceae* (as described above), the *Ruminococcaceae* family represents the highest butyrate-producing bacteria in the gut (Deleu et al., 2021) (Aho et al., 2021). An increase in the abundance of *Oscillospiraceae* and *Rikenellaceae* families has also been linked with higher butyrate production (Louis and Flint, 2017; Tanca et al., 2018), indicating a direct or indirect role of these families in butyrate synthesis pathways as well. Furthermore, the *Rikenellaceae* family is known to have a high number of genes encoding for tryptophanase, an enzyme involved in digesting tryptophan to indole, and may influence MJD development as described above (Jaglin et al., 2018). Overall, the observed decrease in ASVs in the *Lachnospiraceae*, *Ruminococcaceae, Oscillospiraceae* and *Rikenellaceae* and their associations with MJD symptoms may suggest an essential role of these microbes in disease progression. The exact nature of the biological mechanisms involved in these effects remain to be fully understood in relation to MJD development and more broadly neurodegeneration.

4.4. Understanding how changes within the gut microbiota could contribute to disease development and progression

As changes in the gut microbiome have been identified in several neurodegenerative diseases, a range of hypotheses have arisen as to how these may contribute to the development and progression of such diseases. In some forms of neurodegeneration, a role of disease progression through the gut-brain axis has been proposed to be important (Singh et al., 2021). In Parkinson's disease, symptoms such as constipation have been reported to occur before motor symptoms develop, and animal model studies have found that protein aggregates of alpha-synuclein develop within the enteric neurons of the gut may spread to the substantia nigra via anatomically connected neurons (Braak et al., 2006). Further, truncal vagotomy, surgical severing of the vagus nerve, a nerve that links the gut directly to the central nervous system can provide protective effects and is associated with a decreased risk of developing Parkinson's disease (Liu et al., 2017a; Svensson et al., 2015) and dementia (Lin et al., 2018).

Alternative potential mechanisms include the influence of metabolites produced by the gut microbiome that may be taken up by blood circulation or the gut-brain axis. Changes in the concentrations of these metabolites, due to altered abundance and functions of the microbiome producers may have disease modifying effects. Whilst a range of metabolites has been reported to have such effects, we have previously demonstrated that treatment of cellular and zebrafish models of MJD with sodium butyrate can result in beneficial effects such as removal of protein aggregates and decreased motor deficits (Watchon et al., 2021). Similarly, Chou et al. (2011) reported improvements in neurological symptoms (ataxia) and increased survival following the treatment of MJD mice with sodium butyrate.

Finally, additional studies have proposed that alterations in the composition of the gut microbiome may lead to altered levels of important inflammatory modulators. Interestingly, it has been hypothesised that microbial dysbiosis within the gut can alter host cell behaviour, triggering chronic activation of immune or inflammatory responses. Microbial production of SCFAs has been shown to influence the activity of microglia within the central nervous system and thus may indirectly contribute to neuroinflammation and neurodegeneration within the central nervous system through altering microglial maturation and activity. This hypothesis is supported by recent work from Colombo et al. (2021) who reported a decreased presence of amyloid-beta plaques within brain tissue and reduced levels of SCFAs in plasma samples obtained in germ-free transgenic APP/PS1 mice modelling Alzheimer's disease. Further, gut dysbiosis or inflammation within the gut may alter the activity of immune cells within the enteric nervous system, such as muscularis macrophages, which are functionally involved in the clearance of neuronal debris, and thus diminished macrophage function within the gut could contribute to protein aggregation pathology (Singh et al., 2021). Such inflammatory mediators are hypothesised to play a role in the development of neurodegenerative diseases. (Singh et al., 2021).

Our study indicates a plausible role of the gut microbiota in the development or severity of MJD. Many therapeutic strategies that have been explored for the treatment of MJD have failed to yield meaningful improvements in quality of life and lifespan. Expanding the search for therapeutic targets to a broader field, not solely focused on the central

nervous system, may reveal other strategies with therapeutic benefits. Here, we suggest the gut microbiome can be a potential target for developing novel therapies for MJD and highlight the importance of investigating this link further as a means of either delaying the onset or reducing the severity of MJD symptoms.

5. Conclusions

This is the first report demonstrating a potential role of the gut microbiota in MJD development, or the development of spinocerebellar ataxias, more broadly. In addition to MJD-related alterations in the gut microbiota, we report that these changes are present before the onset of any neurological symptoms or motor deficits in both male and female mice. Some of these early microbiota changes were exacerbated at the symptomatic and well-established stages of MJD and could potentially be targeted for therapeutic modulation of the gut microbiota to confer health benefits in MJD. Future studies aimed at altering the gut microbiota through approaches including probiotic, prebiotic and postbiotic supplementation may offer new treatment strategies for MJD. Given pre-symptomatic changes in the gut microbiota, we propose that ameliorating these gut microbiota changes early could potentially delay or reduce the severity of MJD symptoms. Investigation into whether the gut microbiota is also altered in MJD patients will be useful in identifying whether this mechanism is an important regulator of disease development. Further, as MJD is a complex, multifactorial disease, further insight will be useful in identifying whether gut microbiota changes need consideration in disease management or offer an accessible target for therapeutic intervention.

Supplementary data to this article can be found online at https://doi.org/10.1016/j.nbd.2023.106051.

Author contributions

Conceptualization: HG, KR, IP and AL; experiments: HG, KR and LL; analysis: HG, KR and AL; writing—original draft preparation: HG, KR, and AL; writing—review and editing: HG, KR, LL, IP and AL; project administration: HG, KR and AL; funding acquisition: HG and AL. All authors have read and agreed to the published version of the manuscript.

Funding

This research was funded by the MJD Foundation, Australia and NHMRC (grant ID APP2012895), Australia. KR was supported by a Macquarie University Research Excellence Scholarship.

Declaration of Competing Interest

The authors declare no conflict of interest.

Data availability

The 16S rRNA gene sequence data generated and analysed during the current study are available in the GenBank Sequence Read Archive database under accession number PRJNA887924.

Acknowledgements

Fig. 1A and the Graphical Abstract were created with BioRender.com.

References

Adams-Carr, K.L., et al., 2016. Constipation preceding Parkinson's disease: a systematic review and meta-analysis. J. Neurol. Neurosurg. Psychiatry 87, 710–716.
Aho, V.T.E., et al., 2021. Relationships of gut microbiota, short-chain fatty acids, inflammation, and the gut barrier in Parkinson's disease. Mol. Neurodegener. 16, 6.
Amir, A., et al., 2017. Deblur rapidly resolves single-nucleotide community sequence patterns. mSystems 2.
Biagi, E., et al., 2016. Gut microbiota and extreme longevity. Curr. Biol. 26, 1480–1485.
Blacher, E., et al., 2019. Potential roles of gut microbiome and metabolites in modulating ALS in mice. Nature. 572, 474–480.
Bolyen, E., et al., 2019. Reproducible, interactive, scalable and extensible microbiome data science using QIIME 2. Nat. Biotechnol. 37, 852–857.
Braak, H., et al., 2006. Gastric alpha-synuclein immunoreactive inclusions in Meissner's and Auerbach's plexuses in cases staged for Parkinson's disease-related brain pathology. Neurosci. Lett. 396, 67–72.
Burt, T., et al., 1996. Machado-Joseph disease in East Arnhem Land, Australia. Chromosome 14q32.1, 1118–1122 expanded repeat confirmed in four families. 46.
Canani, R.B., et al., 2011. Potential beneficial effects of butyrate in intestinal and extraintestinal diseases. World J. Gastroenterol. 17, 1519–1528.
Challis, C., et al., 2020. Gut-seeded α-synuclein fibrils promote gut dysfunction and brain pathology specifically in aged mice. Nat. Neurosci. 23, 327–336.
Chou, A.H., et al., 2011. HDAC inhibitor sodium butyrate reverses transcriptional downregulation and ameliorates ataxic symptoms in a transgenic mouse model of SCA3. Neurobiol. Dis. 41, 481–488.
Colombo, A.V., et al., 2021. Microbiota-derived short chain fatty acids modulate microglia and promote Aβ plaque deposition. Elife. 10.
Cosma-Grigorov, A., et al., 2020. Changes in gastrointestinal microbiome composition in PD: a pivotal role of covariates. Front. Neurol. 11, 1041.
Costa, M.D.C., Paulson, H.L., 2012. Toward understanding Machado–Joseph disease. Prog. Neurobiol. 97, 239–257.
Cox, L.M., et al., 2021. Gut microbiome in progressive multiple sclerosis. Ann. Neurol. 89, 1195–1211.
Cryan, J.F., et al., 2019. The microbiota-gut-brain Axis. Physiol. Rev. 99, 1877–2013.
D'Abreu, A., et al., 2010. Caring for Machado–Joseph disease: Current understanding and how to help patients. Parkinsonism Relat. Disord. 16, 2–7.
Deleu, S., et al., 2021. Short chain fatty acids and its producing organisms: an overlooked therapy for IBD? EBioMedicine. 66, 103293.
Durr, A., 2010. Autosomal dominant cerebellar ataxias: polyglutamine expansions and beyond. Lancet Neurol. 9, 885–894.
Durr, A., et al., 1996. Spinocerebellar ataxia 3 and Machado-joseph disease: clinical, molecular, and neuropathological features. Ann. Neurol. 39, 490–499.
Fang, X., et al., 2016. Evaluation of the microbial diversity in amyotrophic lateral sclerosis using high-throughput sequencing. Front. Microbiol. 7.
França Jr., M.C., et al., 2010. Clinical correlates of autonomic dysfunction in patients with Machado-Joseph disease. Acta Neurol. Scand. 121, 422–425.
Harrell, F.E.J., 2021. Harrell Miscellaneous. R Package Version 4.6–0. https://hbiostat.org/R/Hmisc/.
He, S., et al., 2021. The gut microbiome and sex hormone-related diseases. Front. Microbiol. 12.
Jaglin, M., et al., 2018. Indole, a signaling molecule produced by the gut microbiota, negatively impacts emotional behaviors in rats. Front. Neurosci. 12.
Jari Oksanen, F., et al., 2019. Vegan: Community Ecology Package. R package.
Jurado-Coronel, J.C., et al., 2018. Sex differences in Parkinson's disease: features on clinical symptoms, treatment outcome, sexual hormones and genetics. Front. Neuroendocrinol. 50, 18–30.
Katoh, K., et al., 2002. MAFFT: a novel method for rapid multiple sequence alignment based on fast Fourier transform. Nucleic Acids Res. 30, 3059–3066.
Kieling, C., et al., 2007. Survival estimates for patients with Machado–Joseph disease (SCA3). Clin. Genet. 72, 543–545.
Klockgether, T., et al., 1998. The natural history of degenerative ataxia: a retrospective study in 466 patients. Brain. 121, 589–600.
Kong, G., et al., 2020. Microbiome profiling reveals gut dysbiosis in a transgenic mouse model of Huntington's disease. Neurobiol. Dis. 135, 104268.
Leotti, V.B., et al., 2021. CAG repeat size influences the progression rate of spinocerebellar Ataxia type 3. Ann. Neurol. 89, 66–73.
Lin, S.-Y., et al., 2018. Dementia and vagotomy in Taiwan: a population-based cohort study. BMJ Open 8, e019582.
Liu, B., et al., 2017a. Vagotomy and Parkinson disease: a Swedish register-based matched-cohort study. Neurology. 88, 1996–2002.
Liu, J., et al., 2017b. Sodium butyrate exerts protective effect against Parkinson's disease in mice via stimulation of glucagon like peptide-1. J. Neurol. Sci. 381, 176–181.
Lo, R.Y., et al., 2016. Depression and clinical progression in spinocerebellar ataxias. Parkinsonism Relat. Disord. 22, 87–92.
Louis, P., Flint, H.J., 2017. Formation of propionate and butyrate by the human colonic microbiota. Environ. Microbiol. 19, 29–41.
Maciel, P., et al., 1995. Correlation between CAG repeat length and clinical features in Machado-Joseph disease. Am. J. Hum. Genet. 57, 54–61.
Martins, S., Sequeiros, J., 2018. Origins and spread of Machado-Joseph disease ancestral mutations events. In: Nóbrega, C., Pereira de Almeida, L. (Eds.), Polyglutamine Disorders. Springer International Publishing, Cham, pp. 243–254.
Mastammanavar, V.S., et al., 2020. Non-motor symptoms in patients with autosomal dominant spinocerebellar ataxia. Acta Neurol. Scand. 142, 368–376.
Nandwana, V., et al., 2022. The role of microbiome in brain development and neurodegenerative diseases. Molecules. 27.
Ngo, S.T., et al., 2020. Progression and survival of patients with motor neuron disease relative to their fecal microbiota. Amyotroph. Lateral. Scler. Frontotemporal. Degener. 21, 549–562.
Nicholson, K., et al., 2021. The human gut microbiota in people with amyotrophic lateral sclerosis. Amyotrophic Lateral Sclerosis Frontotemp. Degenerat. 22, 186–194.
Onofre, I., et al., 2016. Fibroblasts of Machado Joseph disease patients reveal autophagy impairment. Sci. Rep. 6, 28220.

Paulson, H.L., et al., 1997. Intranuclear inclusions of expanded polyglutamine protein in spinocerebellar ataxia type 3. Neuron. 19, 333–344.
Price, M.N., et al., 2010. FastTree 2–approximately maximum-likelihood trees for large alignments. PLoS One 5, e9490.
Qiao, C.M., et al., 2020. Sodium butyrate causes α-synuclein degradation by an Atg5-dependent and PI3K/Akt/mTOR-related autophagy pathway. Exp. Cell Res. 387, 111772.
Quast, C., et al., 2013. The SILVA ribosomal RNA gene database project: improved data processing and web-based tools. Nucleic Acids Res. 41, D590–D596.
Rothhammer, V., et al., 2016. Type I interferons and microbial metabolites of tryptophan modulate astrocyte activity and central nervous system inflammation via the aryl hydrocarbon receptor. Nat. Med. 22, 586–597.
Rothhammer, V., et al., 2018. Microglial control of astrocytes in response to microbial metabolites. Nature. 557, 724–728.
Rowin, J., et al., 2017. Gut inflammation and dysbiosis in human motor neuron disease. Phys. Rep. 5.
Ruano, L., et al., 2014. The global epidemiology of hereditary Ataxia and spastic paraplegia: a systematic review of prevalence studies. Neuroepidemiology. 42, 174–183.
Rüb, U., et al., 2003. Guidelines for the pathoanatomical examination of the lower brain stem in ingestive and swallowing disorders and its application to a dysphagic spinocerebellar ataxia type 3 patient. Neuropathol. Appl. Neurobiol. 29, 1–13.
Rüb, U., et al., 2013. Clinical features, neurogenetics and neuropathology of the polyglutamine spinocerebellar ataxias type 1, 2, 3, 6 and 7. Prog. Neurobiol. 104, 38–66.
Sampson, T.R., et al., 2016. Gut microbiota regulate motor deficits and Neuroinflammation in a model of Parkinson's disease. Cell. 167, 1469–1480.e12.
Savica, R., et al., 2009. Medical records documentation of constipation preceding Parkinson disease: a case-control study. Neurology. 73, 1752–1758.
Scheperjans, F., et al., 2015. Gut microbiota are related to Parkinson's disease and clinical phenotype. Mov. Disord. 30, 350–358.
Schmidt, T., et al., 1998. An isoform of ataxin-3 accumulates in the nucleus of neuronal cells in affected brain regions of SCA3 patients. Brain Pathol. 8, 669–679.
Segata, N., et al., 2011. Metagenomic biomarker discovery and explanation. Genome Biol. 12, R60.
Seidel, K., et al., 2012. Brain pathology of spinocerebellar ataxias. Acta Neuropathol. 124, 1–21.
Shimizu, H., et al., 2010. Involvement of Onuf's nucleus in Machado-Joseph disease: a morphometric and immunohistochemical study. Acta Neuropathol. 120, 439–448.
Silva-Fernandes, A., et al., 2014. Chronic treatment with 17-DMAG improves balance and coordination in a new mouse model of Machado-Joseph disease. Neurotherapeutics. 11, 433–449.
Singh, A., et al., 2021. Neurodegenerative disorders and gut-brain interactions. J. Clin. Invest. 131.
Sittler, A., et al., 2018. Deregulation of autophagy in postmortem brains of Machado-Joseph disease patients. Neuropathology. 38, 113–124.
Svensson, E., et al., 2015. Vagotomy and subsequent risk of Parkinson's disease. Ann. Neurol. 78, 522–529.
Takiyama, Y., et al., 1993. The gene for Machado-Joseph disease maps to human chromosome 14q. Nat. Genet. 4, 300–304.
Tanca, A., et al., 2018. Clostridial butyrate biosynthesis enzymes are significantly depleted in the gut microbiota of nonobese diabetic mice. mSphere. 3.
Teixeira-Castro, A., et al., 2015. Serotonergic signalling suppresses ataxin 3 aggregation and neurotoxicity in animal models of Machado-Joseph disease. Brain. 138, 3221–3237.
Valeri, F., Endres, K., 2021. How biological sex of the host shapes its gut microbiota. Front. Neuroendocrinol. 61, 100912.
Vegeto, E., et al., 2019. The role of sex and sex hormones in neurodegenerative diseases. Endocr. Rev. 41, 273–319.
Vogt, N.M., et al., 2017. Gut microbiome alterations in Alzheimer's disease. Sci. Rep. 7, 13537.
Wang, B., et al., 2020. A high-fat diet increases gut microbiota biodiversity and energy expenditure due to nutrient difference. Nutrients. 12, 3197.
Wasser, C.I., et al., 2020. Gut dysbiosis in Huntington's disease: associations among gut microbiota, cognitive performance and clinical outcomes. Brain Commun. 2.
Watchon, M., et al., 2021. Treatment with sodium butyrate has therapeutic benefits for Machado-Joseph disease through the induction of autophagy. bioRxiv. https://doi.org/10.1101/2021.04.30.442119.
Yamada, M., et al., 2001. Involvement of the cerebral cortex and autonomic ganglia in Machado-Joseph disease. Acta Neuropathol. 101, 140–144.
Yang, F., et al., 2020. Effect of diet and intestinal AhR expression on fecal microbiome and metabolomic profiles. Microb. Cell Factories 19, 219.
Yeh, T.H., et al., 2005. Autonomic dysfunction in Machado-Joseph disease. Arch. Neurol. 62, 630–636.
Zhang, Y., et al., 2022. Sodium butyrate attenuates rotenone-induced toxicity by activation of autophagy through epigenetically regulating PGC-1α expression in PC12 cells. Brain Res. 1776, 147749.
Zhuang, Z.Q., et al., 2018. Gut microbiota is altered in patients with Alzheimer's disease. J. Alzheimers Dis. 63, 1337–1346.